PREDICTING LIMIT CYCLE AMPLITUDES BY COMBINING A HELMHOLTZ SOLVER WITH A FLAME DESCRIBING FUNCTION

R. Kulkarni*[1], F. Nicoud[1]

[1] University Montpellier II, I3M
34095, Montpellier, France
* Corresponding author: kulkarni@math.univ-montp2.fr

The objective of the present study is to investigate whether limit cycle amplitude and frequency can be predicted using a Helmholtz solver. Combustion is modeled by a flame describing function (FDF) so that the unsteady heat release depends on both the angular frequency and the amplitude of the fluctuation. A finite element approach is used to build the finite dimension, algebraic eigenvalue problem corresponding to the wave equation for the pressure fluctuations. An iterative method is used to solve this nonlinear eigenvalue problem in the frequency space. A first comparison between the measured and computed limit cycle is then given.

1 Introduction

Thermoacoustic instabilities result from the coupling between acoustics and combustion [1] and may lead to very large amplitude fluctuations. These high amplitude oscillations can cause structural vibrations, augmented heat fluxes to the chamber walls, reducing the system lifetime and often result into severe damage. The gas turbine manufacturers have devoted large amount of efforts in handling these instabilities. Still, the mechanism is not fully understood and a method which can predict the instability at the design level is required.

A common practice to deal with these kind of instabilities is to model the geometry of the combustor by a network of one or two dimensional axisymmetric acoustic elements where the acoustic problem is solved analytically [1,2]. Jump relations across the compact flame are used to connect these elements by enforcing the pressure continuity and the volume flow rate conservation. The amplitudes of the forward and backward acoustic waves are determined so that the jump relations and the boundary conditions are satisfied. This can only be achieved for a discrete set of angular frequency ω which are the roots of the dispersion relation in the complex plane. The main drawback of this approach is that the geometrical details of a combustor can not be accounted for and only the first "equivalent" longitudinal or orthoradial modes are sought for. Another way is to perform the Large Eddy Simulation (LES) which is a powerful tool to study the dynamics of turbulent flames [1]. However, an important limitation of LES is its cost. The intrinsic nature of LES (full three dimensional resolution of the unsteady Navier Stokes equations) makes it very expensive even on todays computers. Moreover, the instability analysis with LES does not provide any physical reason or a method to control the growing oscillations in the system. Therefore, tools which are faster and which can provide better physical insight of the system dynamics are needed.

One central difficulty in the analysis of combustion instability is the coupling between the acoustics and flame dynamics. Traditionally, the theoretical interpretation is based on the linear stability analysis which examines the growth rate of infinitesimally small perturbations. However, in the real experi-

ments, nonlinearities eventually appear and a limit cycle is reached in a self sustained unstable system. The impact of the nonlinearity in a thermoacoustic system is well documented [3,4,5]. The theoretical investigations of the nonlinearity in the system are roughly divided into two classes. The first group which relies on the Galerkin projection of the modes of the system has been extensively used to investigate nonlinear acoustics as the mechanism responsible for the amplitude saturation [3,4]. In the second class, the models are developed which infer that the combustion is the central nonlinearity [5,6] and responsible for the limit cycle oscillations. The present analysis belong to the second group. The nonlinear investigation performed here is carried out by making use of the describing function framework [6,7].
A proper framework to analyze the combustion instability is the wave equation in reacting flows [1]. Since the characteristic Mach number is very small in practical combustors, the derivation of this equation is usually performed under the zero Mach number assumption. A natural way of gaining information about the whole set of thermoacoustic modes is then to consider harmonic fluctuations and the associated Helmholtz equation. The original initial value problem is then transformed into an eigenvalue problem which can be discretized by using an appropriate finite element method. The shape of the thermoacoustic modes is related to eigenfunctions and their frequencies and growth rates are determined by the eigenvalues. In the presence of combustion, the coupling between the acoustics and the flame makes the eigenvalue problem nonlinear and classical methods cannot be applied to solve the Helmholtz equation [8]. The objective of the present paper is to demonstrate the possibility of using a Helmholtz solver to predict not only the frequency of oscillation and growth rate of a self sustained thermoacoustic system, but also the amplitude of its limit cycle. The rest of the paper is organized as follows. In section 2, a brief description of the Helmholtz solver is given. Further, in section 3, the experimental configuration used for the study is explained. The comparison between experimental results and the present numerical estimates is done in the result section 4.

2 Acoustic solver for the Helmholtz equation

An appropriate framework to study the thermoacoustic instabilities is the wave equation derived under the no mean flow and small amplitude fluctuations assumptions [1]:

$$\nabla.(c_0^2 \nabla p') - \frac{\partial^2 p'}{\partial t^2} = -(\gamma - 1)\frac{\partial q'}{\partial t} \tag{1}$$

where the subscript 0 refers to mean quantities and the superscript "prime" refers to small perturbations. The quantity q' is the local perturbed heat release rate per unit volume and c_0 is the sound speed which can change locally because of changes in temperature.
The acoustic tool used in this study (called AVSP)[8] solves the eigenvalue problem associated to the wave equation. The wave equation (1) is solved in the frequency domain by assuming harmonic variations at a frequency $f = \omega/2\pi$ for pressure, velocity and local heat release perturbations:

$$p' = \hat{P}(x,y,z)\exp(-i\omega t) \qquad u' = \hat{u}(x,y,z)\exp(-i\omega t) \qquad q' = \hat{q}\exp(-i\omega t) \tag{2}$$

No mean flow assumption leads to a linear relationship between the acoustic velocity and pressure given as: $\rho_0 i\omega\hat{\mathbf{u}} = \nabla\hat{P}$. Introducing equation (2) into equation (1) leads to the following Helmholtz equation:

$$\nabla.(c_0^2 \nabla\hat{P}) + \omega^2\hat{P} = i\omega(\gamma - 1)\hat{q} \tag{3}$$

where the unknown quantities are the complex amplitude $\hat{P}$ of the pressure oscillations and angular frequency ω. Note that $\hat{q}$, the complex amplitude of the heat release rate perturbation is also unknown and must be modeled.

2.1 Flame response

Modeling the unsteady behavior of the flame is the most challenging part of the analysis. This is done in AVSP through an extension of the $n-\tau$ model [8].

$$\hat{q}(x) = \frac{q_{av}}{\bar{u}} n_{loc}(x) e^{i\omega\tau(x)} \hat{\mathbf{u}}(\mathbf{x_{ref}}).\mathbf{n_{ref}} \tag{4}$$

where, $\mathbf{n_{ref}}$ is the unit vector defined along the principal axis of the setup oriented towards the burnt gases and $\hat{\mathbf{u}}$ is the acoustic velocity at the reference location x_{ref} upstream of the flame. The scaling by the volume averaged heat release rate (q_{av}) and the bulk velocity ($\bar{u}$) is used to make sure that $n_{loc}(x)$ has no dimensions. In the original $n-\tau$ model [9], the interaction index n and time delay τ are the two parameters describing the acoustic behavior of a compact flame located at position x_{ref}. In the present approach where the geometry of the combustor is fully described, the flame is distributed and the interaction index and time delay depend on space. These data can be extracted either from LES or experimental results. Here, time averaged LES results are used to obtain the required speed of sound distribution $c_0(x)$ while experimentally measured flame describing function is used to determine the flame response. The FDF, which is an extension of the flame transfer function, explicitly quantifies the dependence of the flame response on the angular frequency ω as well as on the amplitude of the perturbations [6,7,10,11]. It is formally expressed as:

$$F(\omega_r, |\hat{u}|) = \frac{\hat{Q}/\bar{Q}}{(\hat{\mathbf{u}}.\mathbf{n_{ref}})/\bar{u}} = G(\omega_r, |\hat{\mathbf{u}}|) e^{i\phi(\omega_r, |\hat{\mathbf{u}}|)} \tag{5}$$

where $\bar{Q}$ is the global heat release rate in the flame (expressed in Watt). However, equation (4) is a pointwise flame model which relates the local heat release rate per unit volume $\hat{q}(x)$ to the reference acoustic velocity. In other words, $\hat{q}(x)$ and q_{av} in equation (4) are expressed in W/m^3. The field of local interaction index $n_{loc}(x)$ is constructed such a way that the expressions (4) and (5) correspond to the same volume integrated flame response. To do so, one assumes that the local interaction index $n_{loc}(x)$ is zero everywhere, except in the flame region where it takes a constant value n_0. Besides, one assumes that the flame is compact enough to state that the local time delay is constant, $\tau_{loc}(x) = \tau$. Equation (4) can then be integrated over the whole volume to give:

$$\int \hat{q}(x) dx = \frac{q_{av} n_0}{\bar{u}} e^{i\omega\tau} \hat{\mathbf{u}}(\mathbf{x_{ref}}).\mathbf{n_{ref}} V_{flame} \tag{6}$$

where V_{flame} is the volume of the reactive zone where the local interaction index equals n_0. In order to ensure that the global flame response from equations (4) and (5) are the same, it is necessary to choose:

$$\tau = \frac{\phi(\omega_r, |\hat{\mathbf{u}}|)}{\omega} \qquad \text{and} \qquad n_0 = \frac{G(\omega_r, |\hat{u}|)\bar{Q}}{q_{av} V_{flame}} \tag{7}$$

The volume and the shape of the reaction zone where the acoustic-flame coupling takes place still need to be defined. In the present study, the flame zone corresponds to the set of positions where the heat release rate $q(x)$ obtained from LES is larger than a user prescribed threshold value "q_{th}". Of course, the reaction zone will be thiner for the larger values of q_{th}. However, n_0 is inversely proportional to V_{flame} (see equation (7)) so that the overall flame response remains consistent with the experimental FDF. The summary of the input and output to the Helmholtz code is given in table 1. The field of interaction index $n_{loc}(x)$ and thus the output are obtained for a fixed value of the perturbation amplitude $|\hat{\mathbf{u}}|$.

2.2 Iterative method

After modeling the unsteady heat release, equation (3) can be converted into matrix form. Knowing the boundary conditions, the speed of the sound distribution and the flame response, a Galerkin finite

Table 1: Input and output of AVSP

AVSP input	from	AVSP output
speed of sound $c_0(x)$	time averaged LES	mode shape $\hat{P}(x)$
reaction zone	time averaged LES	freq of oscillation Re($\frac{\omega}{2\pi}$)
	(threshold value given by user: q_{th})	
interaction index $n_{loc}(x)$	experiment	Growth rate Im(ω)
time delay τ	experiment	

element method is used to transform equation (3) into the algebraic eigenvalue problem of the form [8]

$$A\hat{P} + \omega B(\omega)\hat{P} + \omega^2 C\hat{P} = D(\omega, |\nabla\hat{P}|)\hat{P} \tag{8}$$

where matrix A corresponds to the operator $\nabla.\frac{1}{\rho_0}\nabla$, matrix B accounts the boundary conditions, C is the mass matrix and D depends on the flame model. Note that the latter depends on the amplitude of the perturbation $|\nabla\hat{P}|$ as imposed by the FDF framework. With the zero Mach number linear assumption, the relation $i\omega\hat{\mathbf{u}} = \frac{\nabla\hat{\mathbf{P}}}{\rho_0}$ is used to substitute $|\hat{\mathbf{u}}|$ in equation (5) by $|\nabla\hat{P}|$. Since no general algorithm exists to solve this kind of nonlinear eigenvalue problem, an iterative algorithm must be used. For each amplitude $|\nabla\hat{P}|$, one may iterate on angular frequency to seek for the corresponding frequency and growth rate. Note that this algorithm is already used in the case where the unsteady combustion is modeled under the liner assumption, thanks to a flame transfer function which only depends on ω and not on $|\nabla\hat{P}|$ [8].

$$A\hat{P} + \omega_{k+1}B\hat{P} + \omega_{k+1}^2 C\hat{P} = D(\omega_k)\hat{P} \tag{9}$$

This equation is solved iteratively until the difference $|\omega_{k+1} - \omega_k|$ is less than a prescribed small parameter ϵ. In the FDF framework, the same algorithm can be used for any fixed value of the amplitude $|\nabla\hat{P}|$:

$$A\hat{P} + \omega_{k+1}B\hat{P} + \omega_{k+1}^2 C\hat{P} = D(\omega_k, |\nabla\hat{P}|)\hat{P} \tag{10}$$

The iteration is carried out until ω_{k+1} is very close to ω_k. The amplitude of the limit cycle is then obtained by seeking for the value of $|\nabla\hat{P}|$ such that Im(ω) is zero. In other words, assessing the amplitude of the limit cycle amounts to finding the root of the function:

$$F : |\nabla\hat{P}| \mapsto Im(\omega) = 0 \tag{11}$$

with the solution for ω is the same as for the FTF based algorithm which can be formally given as [8]:
1)Calculate the eigenfrequencies without flame.
2)Set one of the eigenfrequencies as the initial guess (ω_0)
3)Set $D(\omega_0) = 0$ and $k = 1$.
4)Solve equation (9).
5)Assess the error $\eta = |\omega_k - \omega_{k-1}|/|\omega_0|$
6)Iterate on k until η is small enough.

3 Experimental configuration

The configuration used to test the above Helmholtz/FDF approach has been studied at EM2C. Its principle is depicted in figure 1 [10,11,12].

The three main elements of the setup are the swirler, the flame tube and the upstream manifold where premixed air and methane are injected. The flow rotation is generated by the swirler which comprises eight twisted vanes arranged periodically around a central rod (6 mm in diameter). The details of the swirler are given in [11]. Experimental profiles of axial and azimuthal velocities provide an estimate of the swirl number of about 0.55. Two different operating points are considered for the present study. For the first operating point, the flame tube length (l_3) is 100 mm (operating point A) and the

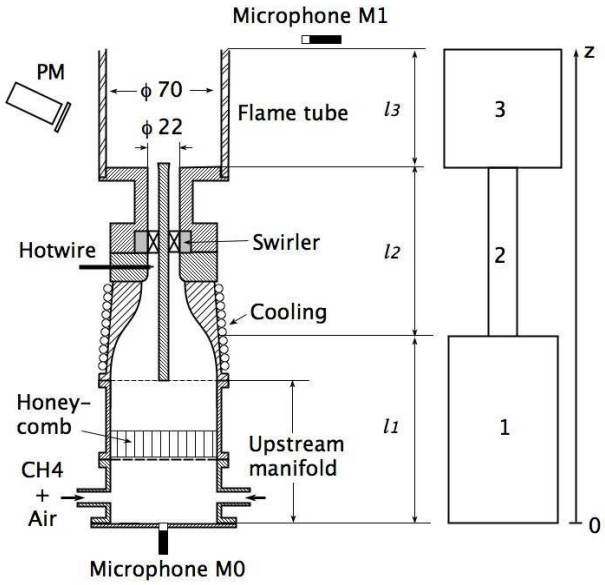

Figure 1: Experimental configuration and its idealized representation. This figure is adopted from [10] with the author's permission.

upstream manifold (l_1) is 117.3 mm (short upstream). The operating point B is for length l_3 = 400 mm and upstream manifold is 181.3 mm (medium upstream). The equivalence ratio is 0.7 and kept constant throughout the analysis and the bulk injection velocity (U_b) is 4.13 m/s.

3.1 Experimental flame describing function

The unsteady heat release rate response is characterized by making use of the describing function [6,7,10,11,12].

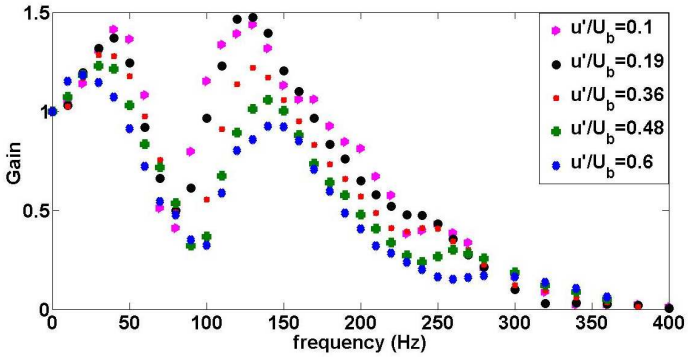

Figure 2: Variation of gain as functions of frequency and ratio of amplitude of root mean square velocity to the bulk velocity u'/U_b. Figure is plotted from [10] with the author's permission.

This quantity, defined by taking the ratio of relative heat release fluctuation to the relative velocity fluctuation, is determined for a range of frequencies and for different levels of incoming velocity perturbations. Velocity perturbations are measured with the hot wire (HW) indicated in figure 1 and heat release rate fluctuations are estimated with photomultiplier equipped with a filter centered on OH^*

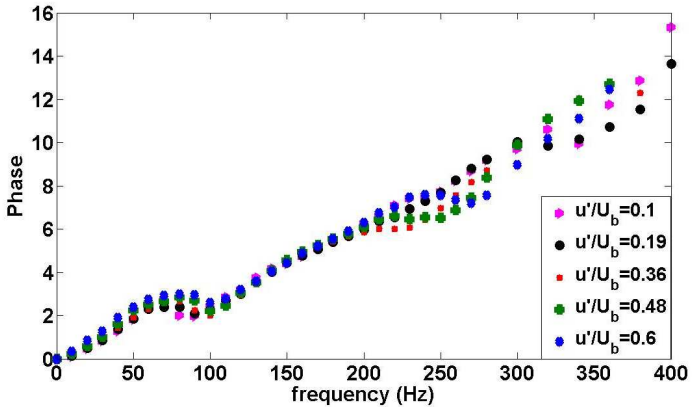

Figure 3: Phase variation as functions of frequency and ratio of amplitude of root mean square velocity to the bulk velocity u'/U_b. Figure is plotted from [10] with the author's permission

emission. As defined in equation (5), the gain reflects the level of the response while the phase defines the time lag between velocity and emission signals. The FDF presented in figure 2 is for bulk velocity U_b = 4.13 m/s over a frequency range of 0 to 400 Hz and for five velocity modulation levels u'/U_b [10,11,12]. The gain approaches one in the low frequency region and the flame acts globally as a low pass filter. The minimum gain is obtained around 90 Hz and maximum gain is obtained around 130 Hz. The phase in figure 3 increases nearly linearly from frequency 0 to 280 Hz [10,11,12]. After 280 Hz, the phase is not smooth due to low value of the gain in this region and the phase becomes difficult to estimate. More details about the features of this FDF can be found in [11].

3.2 Experimental measurement of system damping

The stability of the system is indicated by the sign of the imaginary angular frequency in the absence of the damping. However, real systems always feature some amount of damping α. This quantity is not easy to determine theoretically and is better estimated experimentally [10]. Hence, to determine the stability of the system, the growth rate must be compared with the damping coefficient. The measured value of the damping rate is $\alpha = 55s^{-1}$. It is important to note that the measurement itself is imperfect and features a possible error bar of $\pm 10s^{-1}$ [10]. Stability is then governed by the sign of $\omega_i(|\nabla \hat{P}|) - \alpha$. In other words, when the growth rate $\omega_i(|\hat{\mathbf{u}}|)$ exceeds the damping rate α, the system becomes unstable. Moreover, when $\omega_i(|\hat{\mathbf{u}}|) = \alpha$ the system reaches a limit cycle. This is used to analyze the system stability and the amplitude of the limit cycle.

4 Results and discussion

Two different geometrical configurations are studied in the present analysis. Case 1 corresponds to a short upstream length and a 100 mm flame tube while case 2 corresponds to a medium upstream length and 400 mm flame tube. The authors would like to mention that the calculations are done for the other configurations discussed in [10] as well. However, the focus of the paper is to demonstrate the use of the Helmholtz solver to assess the limit cycle. For the same purpose, only two operating points, one

Table 2: growth rate comparison for case 1 and 2

value of q_{th} (W/m^3)	case 1	case 2
10^4	$\omega_i - \alpha = -41s^{-1}$	$\omega_i - \alpha = 16s^{-1}$
10^8	$\omega_i - \alpha = -41s^{-1}$	$\omega_i - \alpha = 16s^{-1}$

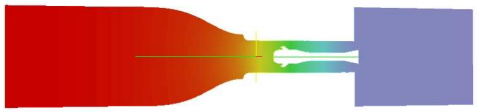

Figure 4: The modulus of the acoustic pressure plotted for the case 1. The maximum and minimum of the pressure occurs at the inlet and outlet respectively.

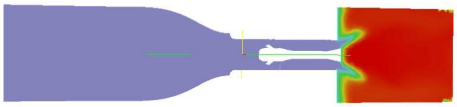

Figure 5: The speed of sound distribution obtained from LES of the reacting flow. The speed of the sound varies from 350 m/s to 830 m/s.

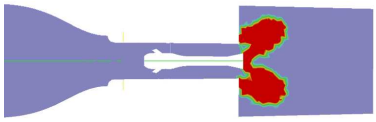

Figure 6: The field of interaction index $n_{loc}(x)$ plotted for a threshold value $10^4 W/m^3$ corresponding to the frequency of 150 Hz and amplitude $\hat{\mathbf{u}}/U_b = 0.1$

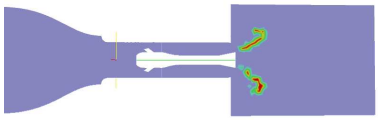

Figure 7: The field of interaction index $n_{loc}(x)$ plotted for a higher threshold value $10^8 W/m^3$. The values of the frequency and the amplitude are same as figure 6.

in the stable and one in the unstable regime, are considered here. Results for both the cases are displayed in Table 2 which shows that case 1 is stable whereas case 2 is not. Note that the values reported in Table 2 were obtained by setting the amplitude to its minimum value $\hat{\mathbf{u}}/U_b = 0.1$. Thus, these results correspond to the classical linear approach where the amplitude effects are not accounted for. This observation matches with the experimental result [10]. For the case 1, $\omega_i - \alpha$ is -41.52s^{-1}. In other words, the growth rate does not exceed the damping rate. Hence, the system is stable for this case. Figure 4 shows the modulus of the acoustic pressure for the quarter wavelength mode for the first case. According to the boundary conditions the pressure is maximum at the inlet ($\hat{\mathbf{u}}$= 0) and minimum at the outlet ($\hat{P} = 0$). Figure 5 shows the sound velocity field obtained from the LES calculation of the reactive flow. The speed of the sound varies from a minimum value of 350 m/s to a maximum value of 830 m/s.
The field of local interaction index is plotted for two different values of threshold for the heat release rate q_{th}. Note that the interaction index field is plotted for the first quarter wavelength mode frequency 150 Hz and the amplitude $\hat{\mathbf{u}}/U_b = 0.1$. Figure 6 shows a thicker flame region with the threshold value 10^4 W/m^3. The interaction index is zero everywhere except in the flame region. The maximum value of $n_{loc}(x)$ in the flame region is 1.8×10^4. The flame is much thinner with the threshold value 10^8 W/m^3 shown in figure 7. The field of interaction index varies from zero to maximum of 2.3×10^5. However, this does not have much impact on the growth rate of the acoustic mode. Even with the thin flame the value of $\omega_i - \alpha$ is -41.52s^{-1}. Since, the system is stable, no additional computations are required in this case.
The growth rate is calculated for the second operating point for a perturbation level $\hat{\mathbf{u}}/U_b = 0.1$. It is observed that, this particular mode is unstable as the value of $\omega_i - \alpha$ is 16.18 s^{-1}. The modulus of the pressure is plotted in figure 8 for case 2 with the flame tube length 400 mm. The maximum and minimum of the acoustic pressure is observed at the inlet and the outlet respectively. Like, the first operating

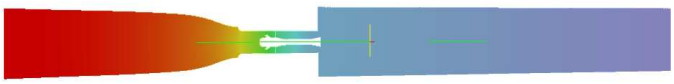

Figure 8: The modulus of the acoustic pressure for the case 2

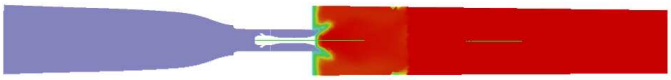

Figure 9: The field of speed of sound obtained from LES for the case 2

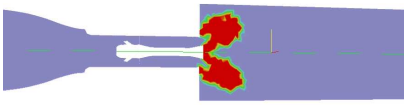

Figure 10: The $n_{loc}(x)$ field for a threshold value $10^4 W/m^3$. The interaction index field is calculated for the frequency 140 Hz and the amplitude $\hat{\mathbf{u}}/U_b = 0.1$

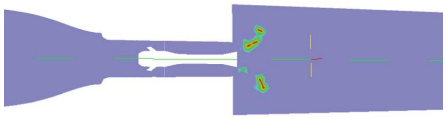

Figure 11: The $n_{loc}(x)$ field for threshold value $10^8 W/m^3$. The value of the frequency and the amplitude is the same as figure 10.

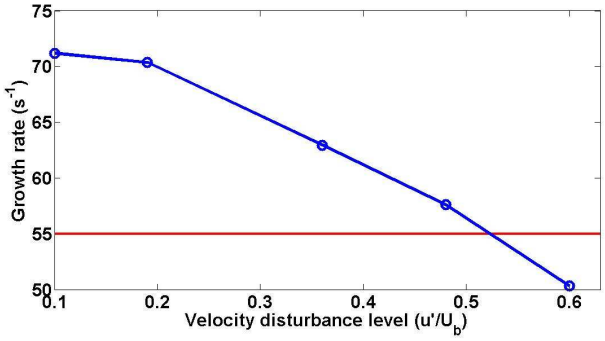

Figure 12: Plot of the growth rate for higher values of the amplitude. It is observed that the limit cycle occurs at an amplitude $\hat{u}/U_b \approx 0.53$

point, the $n_{loc}(x)$ field is plotted for two threshold values corresponding to a thick (figure 10) and the thin flame (figure 11). The frequency is 140 Hz and the amplitude is set to its minimum value $\hat{\mathbf{u}}/U_b = 0.1$ to plot the field of interaction index for the case 2. Besides, $\omega_i - \alpha$ is positive and close to $16 s^{-1}$ in both cases clearly indicating that case 2 is linearly unstable. The next step is to use the Helmholtz/FDF framework to assess the amplitude of the limit cycle. This value is sought for by increasing the amplitude of the perturbations. Experimentally a limit cycle is observed for value $\hat{\mathbf{u}}/U_b \approx 0.7$ [10]. It is observed that the growth rate decreases constantly with increase in the amplitude. This decrease in the growth rate is shown in figure 12. Further, it can be seen that the growth rate crosses the threshold value of the damping in the system at an amplitude $\hat{\mathbf{u}}/U_b \approx 0.53$. In other words, the value of $\omega_i - \alpha$ is zero at this particular amplitude. The experimental value predicts the limit cycle at around $\hat{\mathbf{u}}/U_b \approx 0.7$. In other words, the Helmholtz solver coupled with FDF technique predicts the limit cycle at a value which is close to the experimental result. The frequency of the limit cycle obtained by the algorithm is 139 Hz which is also in good agreement with experimental measurement which indicate 126 Hz.

5 Conclusion

The present study focuses on the use of the Helmholtz solver coupled with the FDF technique to predict the limit cycle amplitude and the frequency. Two different geometrical configurations corresponding to

a swirl stabilized premixed flame are studied. The Helmholtz solver fed by experimental data for the flame response proves able to discriminate between a stable and an unstable configuration. Besides, combining the flame describing function framework with the Helmholtz solver, a fair assessment of the limit cycle corresponding to the unstable case was reached.

Acknowledgments

This study is part of MICCA project supported by the Agence Nationale de la Recherche. The authors are thankful to Paul Palies from Ecole centrale Paris (EM2C laboratory) for giving access to the LES data. Also, the authors would like to express their gratitude to the authorities of the Centre Informatique National de l'Enseignement Superieur (CINES), Montpellier, for the access to the super-computing facilities.

References

[1] T.Poinsot, D. Veynante *Theoretical and numerical combustion*. R. T. Edwards, 2nd Edition, 2005.

[2] S. Stow, A. Dowling *Thermoacoustic oscillations in an annular combustor*. ASME Turbo Expo, 2001-GT-0037, 2001

[3] V. Burnley, F. Culick *On the energy transfer between transverse acoustic modes in a cylindrical combustion chamber*. Combustion Science and Technology, 144, 1-9, 1999

[4] V. Yang, S. I. KIM, F. Culick *Triggering of longitudinal pressure oscillations in combustion chambers 1. nonlinear gas dynamics*. Combustion Science and Technology, 72, 183-214, 1990

[5] A. P. Dowling *A kinematic model of ducted flame*. Journal of fluid mechanics, 394, 51-72, 1999

[6] N. Noiray, D. Durox, T. Schuller, S. Candel *A unified framework for nonlinear combustion instability analysis based on the flame describing function*. Journal of fluid mechanics, 615, 139-167, 2008

[7] N. Noiray, D. Durox, T. Schuller, S. Candel *A method of estimating the noise level of unstable combustion based on the flame describing function*. International Journal of aeroacoustics, 8(1), 157-176, 2009

[8] F. Nicoud, L. Benoit, C. Sensiau, T. Poinsot *Acoustic modes in combustors with complex impedances and multidimensional active flames*. AIAA Journal, 45, 426-441, 2007

[9] L. Crocco *Research on combustion instability in liquid propellant rockets* . 12th Symposium (International) on combustion, Combustion Inst. Pittsburgh, PA, 85-99, 1969

[10] P. Palies, D. Durox, T. Schuller, S. Candel *Swirling flame instability analysis based on the flame describing function methodology*. GT2010-22294, ASME Turbo Expo, June 14-18, Glasgow, United Kingdom 2010

[11] P. Palies, D. Durox, T. Schuller, S. Candel *The combined dynamics of swirler and turbulent premixed swirling flames*. In press, doi:10.1016/Combustion and flame. 2010.02.011

[12] P. Palies, D. Durox, T. Schuller, S. Candel *Combustion instability analysis based on flame describing function applied to swirling flames*. Int'l Summer School and Workshop on Non-normal and Nonlinear effects in Aero- and Thermoacoustics, May 17-21, Munich 2010